

## Prediction of the atomic structure and stability for the ensemble of silicon nanoclusters passivated by hydrogen

This content has been downloaded from IOPscience. Please scroll down to see the full text.

2014 EPL 106 37002

(<http://iopscience.iop.org/0295-5075/106/3/37002>)

View [the table of contents for this issue](#), or go to the [journal homepage](#) for more

Download details:

IP Address: 129.49.235.107

This content was downloaded on 11/07/2014 at 02:22

Please note that [terms and conditions apply](#).

# Prediction of the atomic structure and stability for the ensemble of silicon nanoclusters passivated by hydrogen

V. S. BATURIN<sup>1,3(a)</sup>, S. V. LEPESHKIN<sup>1,3</sup>, N. L. MATSKO<sup>1,3</sup>, ARTEM R. OGANOV<sup>2,3,4</sup> and YU. A. USPENSKI<sup>1</sup>

<sup>1</sup> *P.N. Lebedev Physical Institute, Russian Academy of Sciences - 119991 Leninskii prosp. 53, Moscow, Russia*

<sup>2</sup> *Department of Geosciences, Center for Materials by Design, and Institute for Advanced Computational Science, State University of New York - Stony Brook, NY 11794-2100, USA*

<sup>3</sup> *Moscow Institute of Physics and Technology - Dolgoprudny, Moscow Region 141700, Russia*

<sup>4</sup> *Northwestern Polytechnical University - Xi'an, Shaanxi 710072, PRC*

received 8 December 2013; accepted in final form 10 April 2014  
published online 6 May 2014

PACS 73.22.-f – Electronic structure of nanoscale materials and related systems

PACS 61.46.Bc – Structure of clusters (*e.g.*, metcars; not fragments of crystals; free or loosely aggregated or loosely attached to a substrate)

PACS 64.75.Jk – Phase separation and segregation in nanoscale systems

**Abstract** – The total energy and geometry of nanoclusters  $\text{Si}_{10}\text{H}_{2m}$  ( $m = 0-12$ ) are calculated using evolutionary structure searching and density functional theory. The calculation shows that the arrangement of Si atoms is close to the diamond crystal structure only in the cluster  $\text{Si}_{10}\text{H}_{16}$ , while in others it is unique for each composition. We found that the ensemble of  $\text{Si}_{10}$  clusters remains uniform after passivation only if hydrogen concentration corresponds to one of the stable compositions –  $\text{Si}_{10}$ ,  $\text{Si}_{10}\text{H}_{14}$ ,  $\text{Si}_{10}\text{H}_{16}$ ,  $\text{Si}_{10}\text{H}_{20}$ , or  $\text{Si}_{10}\text{H}_{22}$ . Passivation by an arbitrary amount of hydrogen converts the ensemble into a mixture of the stable clusters having the nearest compositions. In addition there are numerous metastable cluster configurations with energies within  $\sim 0.1$  eV above the ground state. These metastable configurations come into existence in synthesis at  $T \geq 500$  K, making experimentally realizable cluster compositions even more diverse.

Copyright © EPLA, 2014

**Introduction.** – The physical and chemical properties of silicon nanoclusters (Si-NCs) have been subject of extensive research for over two decades. Owing to their strong photoluminescence and their optical spectrum depending on cluster size, geometry and passivation (thus allowing to tune spectra to the desired wavelengths), Si-NCs are considered highly promising for opto- and nanoelectronics, solar cells, biosensors, etc. For applications of Si-NCs in nanodevices, their size and shape should be carefully controlled, since deviations in cluster structure greatly impair working characteristics. Such deviations can originate from both imperfect fabrication technology and intrinsic nanocluster instability. In practice, these two factors are entangled. The situation with instability is more difficult, as in this case even improved fabrication technology will not eliminate the problem.

At present, the atomic structure and stability of Si-NCs are known insufficiently. Most of experimental information relates to small clusters  $\text{Si}_n$  with  $n \leq 10$

(see as examples [1,2]). The search for cluster structure with the lowest energy requires first-principles calculations performed on a large number of atomic configurations. The computational expense grows exponentially with the number of atoms in a cluster; therefore, first-principles studies of larger clusters are usually performed with a symmetry constraint [3] or other extra conditions. Also, there have been many first-principles investigations where the bulk silicon (diamond) structure was used to construct an initial configuration which was relaxed then to the nearest local minimum (see, for instance, [4]). These studies give useful, but fragmentary information on trends in cluster formation, and nearly nothing for Si-NCs ensembles being of importance in many applications.

Our study takes into account the fact that nanoclusters are synthesized in large numbers (ensemble of clusters). Owing to this fact, the system obtains an additional degree of freedom as it can be either uniform (*i.e.* consisting of the same clusters) or non-uniform. In the latter case the system is a mixture of different clusters, which realizes the minimum of ensemble energy. The present

<sup>(a)</sup>E-mail: baturin@lpi.ru

paper considers this problem for the case of a model system consisting of  $\text{Si}_{10}$  nanoclusters passivated by hydrogen of a given concentration. To find the solution for any arbitrary  $\text{H}_2$  concentration, we calculate the atomic structure and energy of all nanoclusters belonging to the set  $\text{Si}_{10}\text{H}_{2m}$  ( $0 \leq m \leq 12$ ). Structure searches for isolated clusters with given composition are performed using an *ab initio* evolutionary algorithm. In addition to the ground-state configurations, the evolutionary algorithm provides a large number of low-energy isomer structures. This information allows us to find the equilibrium constitutions of cluster ensembles at zero temperature and to consider their changes with temperature.

**Computational techniques.** – The computational scheme used here for predicting the optimal atomic structure of an isolated  $\text{Si}_{10}\text{H}_{2m}$  cluster is based on the evolutionary algorithm/code USPEX [5,6]. A search algorithm is briefly described as follows. In the first generation, we initialize the simulation by creating a large number of random symmetric structures; these belong to randomly selected point groups (the number of possible point groups is in principle infinite, but here for the initialization we use all 32 crystallographic point groups, and pentagonal, decagonal and icosahedral groups), with atoms occupying random positions within an ellipsoidal region. All initially produced structures, even before relaxation, are made with full connectivity (that is, all atoms of the cluster participate in the same network of strong bonds) and the volume of the ellipsoidal region approximately corresponds to the expected volume of the cluster. These initially produced clusters are relaxed, and then ranked by energy – a certain share (usually around 40%) of clusters that have the highest energy is discarded, while the rest are allowed to produce the next generation using heredity, shape mutation, soft-mode mutation and permutation [7]. Already at the stage of relaxation, using small perturbations of the structure, symmetry breaking is allowed. These perturbations nudge the structure to relax down the total energy slope to the nearest energy minimum, away from maxima or saddle points. Furthermore, variation operators (heredity and mutations) break symmetry. At the end of each generation, a few distinct structures with the lowest energy are selected as the elite and go to the next generation unchanged. This procedure is looped and terminated when the lowest-energy structure remains unchanged for a sufficiently large number of generations.

During the search, we calculated the total energy and forces within the generalized gradient approximation (GGA) [8] of the density functional theory, as implemented in the Quantum Espresso code [9]. We used the supercell with the lattice parameter of 23.8 Å and plane-wave basis set with the kinetic energy cutoff of 20 Ry and Troullier-Martins norm-conserving pseudopotentials [10]. Self-consistency was considered achieved when the total energy changes were within  $3 \cdot 10^{-4}$  Ry, and relaxation was stopped when forces were less than  $3 \cdot 10^{-3}$  Ry/ $r_B$ . Results

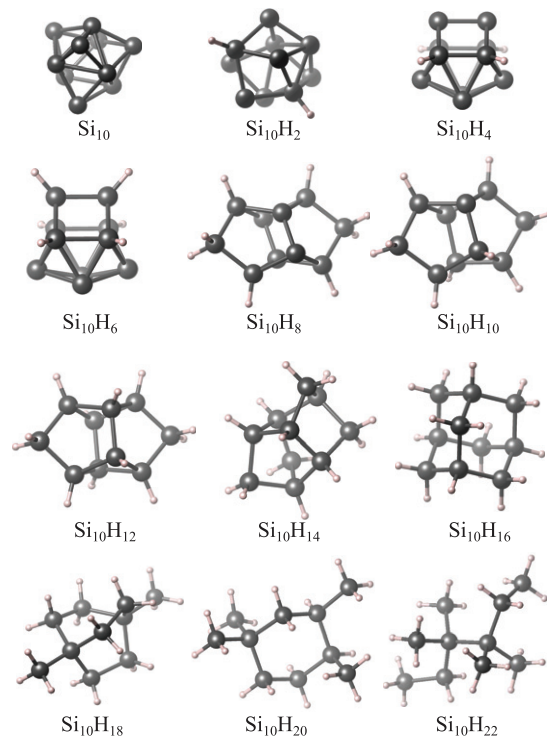


Fig. 1: (Colour on-line) Ground-state structures of  $\text{Si}_{10}\text{H}_{2m}$  clusters ( $0 \leq m \leq 11$ ).

of each evolutionary search were analyzed, a group of low-energy configurations was selected and subsequently relaxed with higher precision: in these calculations, we used the plane-wave cutoff energy of 50 Ry, the total energy precision of  $2 \cdot 10^{-4}$  Ry, and relaxation was performed until the forces acting on atoms were below  $2 \cdot 10^{-4}$  Ry/ $r_B$ . These results gave us the most stable cluster configuration for each  $\text{Si}_{10}\text{H}_{2m}$  composition, and that information was used in further analysis.

**The stability of isolated  $\text{Si}_{10}\text{H}_{2m}$  clusters.** – Our calculations of isolated clusters  $\text{Si}_{10}\text{H}_{2m}$  showed that clusters with  $0 \leq m \leq 11$  are stable against dehydrogenation and their ground-state structures are all very different (fig. 1).

Our pyramidal structure of  $\text{Si}_{10}$  has been identified in the experiment [2]. The sila-adamantane structure of  $\text{Si}_{10}\text{H}_{16}$  is the only one derived from the bulk silicon (diamond-type structure). It is still not observed in experiment, despite the existence of two analogs: the adamantane structure of  $\text{C}_{10}\text{H}_{16}$  [11] and recently synthesized sila-adamantane structure, where atoms H are substituted by methyl and trimethylsilyl groups [12]. The synthesis of  $\text{Si}_{10}\text{H}_{22}$  clusters has been reported [13], but their structure and the structure of other clusters were not determined experimentally. In general, the structures of  $\text{Si}_{10}\text{H}_{2m}$  clusters are quite different from the structures of hydrocarbons: there is a greater variability of local environments in hydrosilicons. Compared to carbon atoms, silicon atoms are much less prone to form double and triple

bonds, and more prone to forming delocalized and less directional bonds. Among cluster structure predictions, we note the genetic algorithm calculations [14]. Their ground-state structures of  $\text{Si}_{10}\text{H}_{12}$ ,  $\text{Si}_{10}\text{H}_{14}$  and  $\text{Si}_{10}\text{H}_{16}$  clusters are identical to those in fig. 1. However, the structures of  $\text{Si}_{10}\text{H}_4$ ,  $\text{Si}_{10}\text{H}_8$  and  $\text{Si}_{10}\text{H}_{20}$  are different. We compared energies of differing structures with our results and found that our structures are lower in energy by 0.03–0.05 eV.

**Equilibrium state of a cluster ensemble.** – In this section we consider the ensemble of clusters  $\text{Si}_{10}\text{H}_{2m}$ , which has, on average,  $N(\text{H}_2)$  hydrogen molecules per  $\text{Si}_{10}$  cluster. The number  $N(\text{H}_2)$  (non-integer, in general) includes both  $\text{Si}_{10}$ -bonded and free  $\text{H}_2$  molecules. The aim here is to find the equilibrium ensemble constitution at given hydrogen concentration  $N(\text{H}_2)$ . As the cluster  $\text{Si}_{10}\text{H}_{24}$  is unstable against dehydrogenation, the constituents of a cluster ensemble with  $N(\text{H}_2) > 11$  are obvious, namely, the  $\text{Si}_{10}\text{H}_{22}$  clusters and free  $\text{H}_2$  molecules. At lower hydrogen concentrations  $N(\text{H}_2) \leq 11$  ensemble constituents are not so trivial, and a special analysis is needed. In this analysis, for simplicity and certainty, we assumed zero interaction between clusters in the ensemble. At zero temperature, possible constituents of the ensemble are cluster structures, with the lowest total energy, which we discussed in the previous section. Their abundances in the ensemble are determined by the minimum of ensemble energy. At finite temperature  $T$ , possible ensemble constituents are the stable cluster structures and metastable isomer structures, whose energy is above the ensemble ground state by  $\Delta E_{\text{tot}} \leq k_{\text{B}}T$ . This fact defines a richer ensemble constitution at elevated temperatures and requires a more sophisticated analysis of ensemble constituents. We determine them from the minimum of ensemble free energy using the Boltzmann statistics.

*A) Ensemble constituents at zero temperature.* We consider the ensemble of  $N$  clusters ( $N \gg 1$ ), which has, on average,  $N(\text{H}_2)$  hydrogen molecules per cluster. The total ensemble energy at zero kelvin is

$$E_{\text{tot}} = \sum_{m=0}^M \varepsilon_0(m) N_m. \quad (1)$$

Here  $\varepsilon_0(m)$  is the minimum energy of a  $\text{Si}_{10}\text{H}_{2m}$  cluster,  $N_m = NC_m$  is the number of  $m$ -type clusters in the ensemble, and  $M = 11$ . The concentrations  $C_m$  (ensemble constituents) are constrained by obvious conditions: they are non-negative real numbers and maintain the total number of clusters  $\text{Si}_{10}$  ( $N = \sum N_m$ ) and the total number of hydrogen molecules ( $NN(\text{H}_2) = \sum m N_m$ ). These conditions are expressed by the equations

$$1 = \sum_{m=0}^M C_m, \quad N(\text{H}_2) = \sum_{m=0}^M m C_m. \quad (2)$$

These constraints define a feasible range of  $C_m$ , where the minimum of  $E_{\text{tot}}$  is searched. However, eq. (1) is not

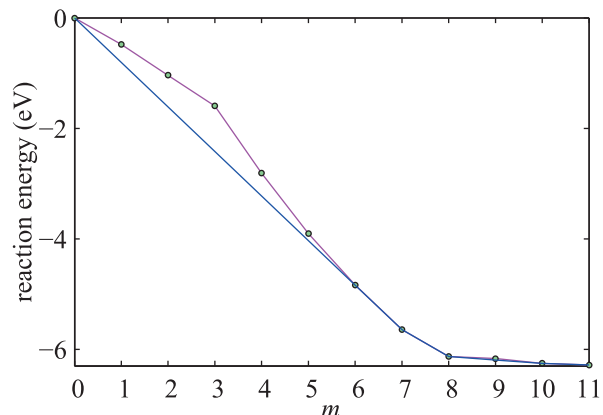


Fig. 2: (Colour on-line) Calculated reaction energy  $\varepsilon_{\text{R}}$  of the ensemble as a function of  $N(\text{H}_2) = m$  (solid line) in comparison with the reaction energy of isolated clusters  $\varepsilon_{\text{R}}(m)$  (linked symbols).

convenient for use, as the energies  $\varepsilon_0(m)$  contain large constant contributions which mask the effect of passivation. For this reason, instead of  $E_{\text{tot}}$ , we minimized the energy of hydrogenation reaction  $\varepsilon_{\text{R}}$ , which differs from  $E_{\text{tot}}$  by the factor  $1/N$  and a constant independent on  $C_m$ :

$$\varepsilon_{\text{R}} = E_{\text{tot}}/N - \varepsilon_0(m=0) - N(\text{H}_2)\varepsilon_0(\text{H}_2) = \sum_{m=0}^M \varepsilon_{\text{R}}(m) C_m, \quad (3)$$

where  $\varepsilon_{\text{R}} = \varepsilon_0(m) - \varepsilon_0(m=0) - N(\text{H}_2)\varepsilon_0(\text{H}_2) \leq 0$  is the energy of hydrogenation reaction in the  $m$ -sort cluster. The minimization of  $\varepsilon_{\text{R}}$  provides ensemble constituents  $C_m$  which are identical to those obtained by the minimization of  $E_{\text{tot}}$ , but allows more transparent interpretation.

It should be noted that the reaction energy  $\varepsilon_{\text{R}}$  (3) is a linear function of  $C_m$ . For this reason its minimum is obtained at the boundary of the feasible range of  $C_m$  defined by the conditions eq. (2). As these conditions are also linear in  $C_m$ , the minimization of (3) with respect to  $M + 1$  concentrations  $C_m$  under constraints (2) is a standard problem of linear programming. To find the minimum, we used the interior point method [15], which is suitable for the solution of both linear and nonlinear convex optimization problems. Figure 2 presents the calculated minimum of the ensemble reaction energy  $\varepsilon_{\text{R}}$  as a function of  $N(\text{H}_2) = m$  in comparison with the reaction energies of isolated clusters  $\varepsilon_{\text{R}}(m)$ .

One can see that the equilibrium ensemble can contain only the following clusters:  $\text{Si}_{10}$  and  $\text{Si}_{10}\text{H}_{14}$  ( $0 < N(\text{H}_2) < 7$ ),  $\text{Si}_{10}\text{H}_{14}$  and  $\text{Si}_{10}\text{H}_{16}$  ( $7 < N(\text{H}_2) < 8$ ),  $\text{Si}_{10}\text{H}_{16}$  and  $\text{Si}_{10}\text{H}_{20}$  ( $8 < N(\text{H}_2) < 10$ ),  $\text{Si}_{10}\text{H}_{20}$  and  $\text{Si}_{10}\text{H}_{22}$  ( $10 < N(\text{H}_2) < 11$ ). Other  $\text{Si}_{10}\text{H}_{2m}$  clusters have higher reaction energies than the mixture of the stable clusters mentioned above and therefore do not appear at  $T = 0\text{K}$ . This is seen in fig. 3, which shows the calculated ensemble constituents at variable hydrogen concentrations

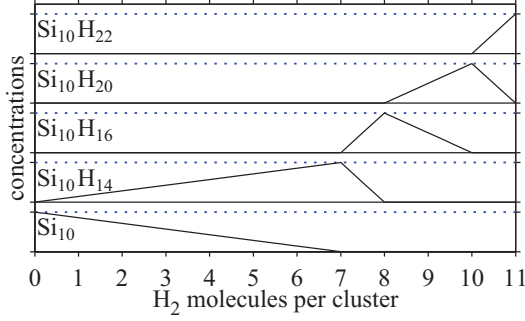


Fig. 3: (Colour on-line) Equilibrium ensemble constituents at  $T = 0$  K as functions of  $N(\text{H}_2)$  (ranging from 0 (solid horizontal lines) to 1 (dotted lines)).

( $0 < N(\text{H}_2) < 11$ ). In the intervals of  $N(\text{H}_2)$ , where the mixture of stable clusters provides the lowest energy, the ensemble constituents  $C_m$  change linearly with  $N(\text{H}_2)$ .

Behavior of the ensemble at low hydrogen concentration ( $0 < N(\text{H}_2) < 7$ ) can be qualitatively explained in terms of dangling bonds. In bare or slightly passivated Si-NCs, the atomic structure, where each silicon atom has four single bonds, is impossible. Electrons that do not participate in bonds occupy dangling bond orbitals and do not favour the stabilization of the structure. For this reason the number of dangling bonds in stable clusters should be minimal. The clusters  $\text{Si}_{10}\text{H}_{2m}$  with  $0 \leq m < 6$  have a significant number of dangling bonds and therefore they drop out of the ensemble. The calculated HOMO-LUMO gaps of stable clusters, which contribute to the ensemble at ( $0 < N(\text{H}_2) < 7$ ), are very different:  $E_g(\text{Si}_{10}) = 2.1$  eV and  $E_g(\text{Si}_{10}\text{H}_{14}) = 3.8$  eV. This leap of  $E_g$  illustrates changes in electronic structure entailed by the complete removal of dangling bonds.

*B) Ensemble constituents at finite temperature.* The analysis of ensemble constituents at finite temperature requires, generally speaking, the consideration of all atomic configurations having energy of  $\sim k_B T$  above the ground state. Such configurations can relate to atomic vibrations, structural and stereo isomers. Estimating the contribution of atomic vibrations in clusters  $\text{Si}_{10}\text{H}_{2m}$ , we note that their energies have two scales: the characteristic temperature of Si-Si bond vibrations is  $\theta_{\text{Si-Si}} \approx 500$  K, while the characteristic temperature of Si-H bond vibrations is much higher,  $\theta_{\text{Si-H}} \geq 1100$  K. This estimate is valid for most related materials, for example, bulk silicon, silane ( $\text{SiH}_4$ ) and disilane ( $\text{Si}_2\text{H}_6$ ) molecules, etc. Here we consider the practically most interesting case where the temperature  $T$  of the ensemble formation falls in the gap between two characteristic temperatures,  $\theta_{\text{Si-Si}} \leq T \ll \theta_{\text{Si-H}}$ . In this case, the contribution of Si-Si vibrations to the ensemble free energy is estimated from the law of equipartition as  $F_{\text{vibr}}(\text{Si-Si}) \approx -N \cdot 10 \cdot 3 \cdot k_B T \ln(T/\theta_{\text{Si-Si}})$ , while the contribution of Si-H vibrations is exponentially small and may be neglected. This estimate shows that the contribution

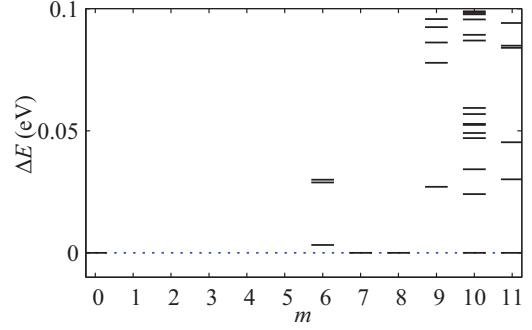


Fig. 4: (Colour on-line) The total energies of low-energy isomer structures for the clusters  $\text{Si}_{10}\text{H}_{2m}$  with  $0 \leq m \leq 11$  given in reference to the average reaction energy of the ensemble at  $T = 0$  K.

of atomic vibrations  $F_{\text{vibr}}$  is roughly independent on the sort of  $\text{Si}_{10}\text{H}_{2m}$  clusters and, hence, has little influence on the ensemble constituents  $C_m$ . Stereoisomers are most difficult for consideration as their bond topology is identical to that of the ground-state structure. In the following, we restrict ourselves to the consideration of structural isomers; which have dissimilar bond topologies and may be easily recognized among candidate structures using spectral graph theory [16]. Figure 4 presents the energies of low-lying structural isomers for all  $\text{Si}_{10}\text{H}_{2m}$  clusters with  $0 \leq m \leq 11$  counted off from the ensemble average reaction energy at  $T = 0$  K. It is seen that the number of structural isomers with low energy is significant, especially for clusters  $\text{Si}_{10}\text{H}_{18}$ ,  $\text{Si}_{10}\text{H}_{20}$  and  $\text{Si}_{10}\text{H}_{22}$ , so their contribution to the ensemble free energy must be important. The  $\text{Si}_{10}\text{H}_{2m}$  clusters with  $1 \leq m \leq 5$  also have low-lying structural isomers; however, their ground-state energies are well above the ensemble energy, and therefore, the energies of these clusters are absent in fig. 4.

Taking into account these points, we determine the ensemble constituents  $C_m$  from the minimum of free energy, where the excited states of clusters  $\text{Si}_{10}\text{H}_{2m}$  correspond to their structural isomers. As interactions between clusters were assumed to be zero, the ensemble free energy is the sum of the free energies related to  $m$ -type clusters, and in the Boltzmann approximation it is equal to

$$F_{\text{tot}} = -k_B T \sum_{m=0}^M N_m \ln \left\{ \frac{e}{N_m} \sum_{i=0} \exp[-\varepsilon_i(m)/(k_B T)] \right\}, \quad (4)$$

where  $\varepsilon_i(m)$  is the energy of the  $i$ -th structural isomer for the  $m$ -sort clusters and  $i = 0$  relates to the ground-state structure of clusters. It is convenient to rewrite this equation subtracting the ground-state energies of initial ensemble components ( $\text{Si}_{10}$  clusters and  $\text{H}_2$  molecules) and multiplying the result by  $1/N$ , as was done in (3):

$$f_R = F_{\text{tot}}/N - \varepsilon_0(m=0) - N(\text{H}_2)\varepsilon_0(\text{H}_2) = \sum_{m=0}^M C_m [\varepsilon_R(m, T) + k_B T \ln C_m] + k_B T \ln \frac{N}{e}. \quad (5)$$

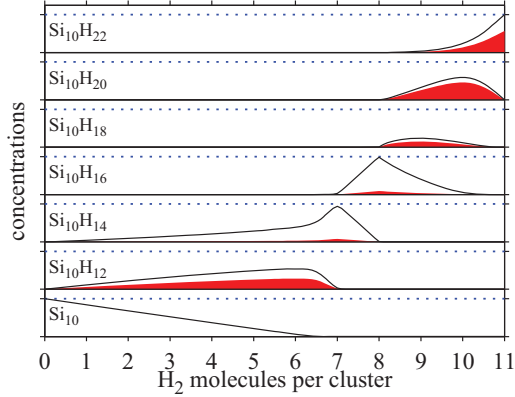


Fig. 5: (Colour on-line) Equilibrium ensemble constituents  $C_m$  at  $T = 500$  K as functions of  $N(\text{H}_2)$ . The height indicates the values of  $C_m$  (ranging from 0 (solid horizontal lines) to 1 (dotted lines)). The filled area shows the respective share of isomer structures.

Separating out the contribution of ground-state structures and denoting  $\Delta_i(m) = \varepsilon_i(m) - \varepsilon_0(m)$ , we obtain the expression for the free energy of hydrogenation reaction:

$$\varepsilon_{\text{R}}(m, T) = \varepsilon_{\text{R}}(m) - k_{\text{B}}T \ln \left\{ 1 + \sum_{i=0} \exp[-\Delta_i(m)/(k_{\text{B}}T)] \right\}. \quad (6)$$

The minimum of  $f_{\text{R}}$  (5) under the constraints eq. (2) determines the ensemble constituents  $C_m$  at temperature  $T$ . To calculate this minimum numerically, we used the interior point method, which has been applied above for  $T = 0$  K.

The results of calculation for  $T = 500$  K are presented in fig. 5. The calculated dependences  $C_m(N(\text{H}_2))$  are similar to those for  $T = 0$  K (fig. 3), but are not identical to them. The first evident distinction is the occurrence of the clusters  $\text{Si}_{10}\text{H}_{12}$  ( $0 < N(\text{H}_2) < 7$ ) and  $\text{Si}_{10}\text{H}_{18}$  ( $8 < N(\text{H}_2) < 11$ ), which do not appear in the ensemble at zero temperature. This occurrence, in turn, decreases distinctly the abundances of the clusters  $\text{Si}_{10}\text{H}_{14}$ ,  $\text{Si}_{10}\text{H}_{16}$ ,  $\text{Si}_{10}\text{H}_{20}$  and  $\text{Si}_{10}\text{H}_{22}$ . The second distinction is a large share of isomer structures in the ensemble. They dominate in clusters  $\text{Si}_{10}\text{H}_{12}$ ,  $\text{Si}_{10}\text{H}_{18}$ ,  $\text{Si}_{10}\text{H}_{20}$  and  $\text{Si}_{10}\text{H}_{22}$ .

The third distinction caused by elevated temperature, which is not seen in fig. 5 is a minor admixture of all clusters to the ensemble. These finer changes are demonstrated in fig. 6, where the concentrations  $C_m$  corresponding to  $T = 500$  K and  $N(\text{H}_2) = 8$  are shown on a logarithmic scale. One may see that the concentration  $C_8$  (of  $\text{Si}_{10}\text{H}_{16}$ ) is still very close to 1.0; however, other  $C_m$  are non-zero and range from  $10^{-6}$  to  $10^{-2}$ . This means that the elevated temperature breaks the ensemble uniformity which is possible at  $T = 0$  K. To understand this important point, we turn to analytic treatment.

The free energy of reaction  $f_{\text{R}}$  (5) is not a linear function of  $C_m$ , as it includes the entropy term  $k_{\text{B}}T \sum C_m \ln C_m$ .

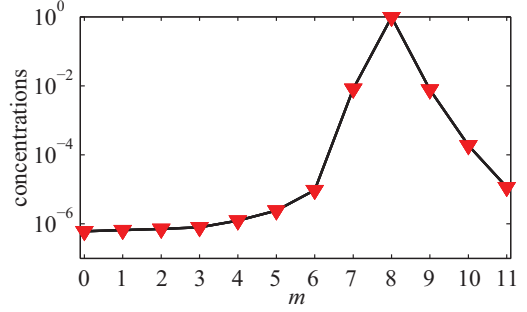


Fig. 6: (Colour on-line) The concentration of clusters  $\text{Si}_{10}\text{H}_{2m}$  in the ensemble at  $T = 500$  K for the average hydrogen concentrations  $N(\text{H}_2) = 8$ .

Because of limitations  $0 \leq C_m \leq 1$ , this term is negative. It shifts the minimum of  $f_{\text{R}}$  from the boundary (at  $T \rightarrow 0$  K) to the inside of a feasible region of  $C_m$ , where its position is determined by the extremum condition  $df_{\text{R}}/dC_m = 0$ . Only  $M - 1$  concentrations are independent, while two, for example  $C_{m'}$  and  $C_{m''}$  are defined by them through eqs. (2). Thus, the equilibrium concentrations  $C_m$  ( $m \neq m', m''$ ) are given by equations

$$0 = \frac{\partial f_{\text{R}}}{\partial C_{m'}} \frac{\partial C_{m'}}{\partial C_m} + \frac{\partial f_{\text{R}}}{\partial C_{m''}} \frac{\partial C_{m''}}{\partial C_m} + \frac{\partial f_{\text{R}}}{\partial C_m}. \quad (7)$$

Here the partial derivatives of  $f_{\text{R}}$  are

$$\frac{\partial f_{\text{R}}}{\partial C_m} = \varepsilon_{\text{R}}(m, T) + k_{\text{B}}T(\ln C_m + 1) \quad (8)$$

After simple algebra equations, eqs. (2) provide

$$\frac{\partial C_{m'}}{\partial C_m} = -\frac{m'' - m}{m'' - m'}, \quad \frac{\partial C_{m''}}{\partial C_m} = -\frac{m - m'}{m'' - m'}. \quad (9)$$

Equations (7)–(9) determine ensemble constituents  $C_m$  at finite  $T$ . They may be solved easily if  $N(\text{H}_2) = m_0$ , where  $m_0$  corresponds to a uniform ensemble at  $T = 0$  K. In this case we may assume that only concentrations  $C_{m_0-1}$ ,  $C_{m_0}$ , and  $C_{m_0+1}$  are non-zero. For this special case, eqs. (2) provide  $C_{m_0-1} = C_{m_0+1} = s/2$  and  $C_{m_0} = 1 - s$ , where  $s$  is given by (7)–(9) as

$$s = \frac{1}{1 + 0.5 \exp[\Delta/(2k_{\text{B}}T)]} \approx 2 \exp[-\Delta/(2k_{\text{B}}T)], \quad (10)$$

$$\Delta = \varepsilon_{\text{R}}(m_0 + 1, T) + \varepsilon_{\text{R}}(m_0 - 1, T) - 2\varepsilon_{\text{R}}(m_0, T). \quad (11)$$

This analytical estimate is rather accurate. For  $N(\text{H}_2) = 8$  the interior point method gives the concentrations  $C_7 = 8.1 \cdot 10^{-3}$ ,  $C_9 = 7.8 \cdot 10^{-3}$ , and  $C_8 = 0.9838$ , while eq. (10) provides  $C_7 = C_9 = 7.9 \cdot 10^{-3}$  and  $C_8 = 0.9842$ . Equation (10) shows that the stability of a cluster ensemble at elevated temperature is defined by the sign and value of  $\Delta$  which is the central difference approximation of the second derivative of  $\varepsilon_{\text{R}}(m, T)$  over  $m$ . This criterion is close to the condition of system resistance to diffusion, which is defined by the second derivative of entropy over concentration [17].

**Discussion and conclusions.** – Our first-principles evolutionary calculations showed that the ground-state atomic structures of  $\text{Si}_{10}\text{H}_{2m}$  clusters with  $0 \leq m \leq 11$  show great variability. Among them only the cluster  $\text{Si}_{10}\text{H}_{16}$  has configuration close to the diamond-type structure of bulk silicon. Our studies revealed that only the clusters  $\text{Si}_{10}$ ,  $\text{Si}_{10}\text{H}_{14}$ ,  $\text{Si}_{10}\text{H}_{16}$ ,  $\text{Si}_{10}\text{H}_{20}$  and  $\text{Si}_{10}\text{H}_{22}$  can exist in the ensemble at  $T = 0$  K (a particular selection of one or two stable clusters from this list depends on the average hydrogen concentration  $N(\text{H}_2)$ ). Because a small amount of hydrogen cannot passivate all dangling bonds, clusters  $\text{Si}_{10}\text{H}_{2m}$  with small  $m$  have rather high energies and drop out of the ensemble. In some sense, the formation of a proper cluster mixture in the ensemble is similar to phase segregation in bulk alloys. We also found that the ensemble behavior is strongly affected by numerous low-energy isomers, which emerge in the ensemble with significant abundances even at the moderate temperature  $T = 500$  K. These facts indicate that the Si-NCs ensembles are nearly uniform in structure and composition only in narrow concentration intervals near the “magic” clusters. In our calculation, one such interval exists near the composition  $\text{Si}_{10}\text{H}_{16}$ , as this cluster possesses both necessary properties: it holds stable in the ensemble and has no low-lying isomers. However, even when the  $\text{H}_2$  concentration exactly corresponds to the  $\text{Si}_{10}\text{H}_{2m}$  composition, the ensemble is not perfectly uniform at  $T = 500$  K, but contains about 1.6% of other clusters. Non-uniformity greatly affects the ensemble properties. For illustration, the HOMO-LUMO gap of  $\text{Si}_{10}$ ,  $\text{Si}_{10}\text{H}_{12}$  and  $\text{Si}_{10}\text{H}_{14}$  (given by DFT) is 2.1 eV, 3.5 eV and 3.8 eV, and only these clusters are in the ensemble at  $0 < N(\text{H}_2) < 7$  and  $T = 500$  K. In such ensemble, the optical gap relating to the absorption edge is 2.1 eV, while the gap measured by a local probe (say, by the STM) takes the values 2.1 eV, 3.5 eV or 3.8 eV, depending on the STM tip position. These data may be considered as contradictory, if ensemble constituents are unknown.

Our analysis here was restricted to the Si-NCs with ten silicon atoms. The full analysis of the Si-NCs ensemble should include clusters with a variable number of Si atoms. This new degree of freedom would lower the relative stability of clusters in the ensemble, because it provides additional ways for mixture formation. It would further restrict chemical composition intervals, where the ensemble of Si-NCs is uniform. As for the ensemble of moderately large clusters (with a diameter of few nanometers), it looks probable that the trends in cluster stability outlined above will remain the same. Of course, in large clusters the atomic structure of the cluster core is close to that of bulk silicon and changes only slightly with cluster size and chemical composition. By contrast, the atomic structure of the cluster shell is sensitive to passivation and can be easily modified. Variations in the shell can provide irregularity in the ensemble composition. Numerous complicated structures observed on the surface

of solids provide indirect indication that such scenario is realistic.

The data on isomers and ground-state structures calculated here —reaction energies, total and relative energies, atomic coordinates and structure figures— can be found in the supporting information file at <http://td.lpi.ru/%7Ebaturin/suppinfo.pdf>.

\*\*\*

This research was supported in part by the Programmes of the Russian Academy of Sciences and the Russian Foundation for Basic Research (grants 13-02-00655, 12-02-31638, 12-02-31774 and 11-02-00615). ARO acknowledges funding from DARPA (Nos. W31P4Q1210008 and W31P4Q1310005), NSF (Nos. EAR-1114313, DMR-1231586), CRDF Global (UKE2-7034-KV-11), and the Government of the Russian Federation (No. 14.A12.31.0003). Calculations were performed at the Joint Supercomputer Center (Russian Academy of Sciences, Moscow, Russia). USPEX code, with options for global optimization of stability of physical properties of crystals, surfaces, polymers, and nanoparticles, is available at <http://uspex.stonybrook.edu>.

## REFERENCES

- [1] HONEA E. C. *et al.*, *J. Chem. Phys.*, **110** (1999) 12161.
- [2] HAERTELT M. *et al.*, *J. Chem. Phys.*, **136** (2012) 064301.
- [3] JUG K., SCHLUFF H.-P., KUPKA H. and IFFERT R., *J. Comput. Chem.*, **9** (1988) 803.
- [4] MITAS L. *et al.*, *Appl. Phys. Lett.*, **78** (1988) 1918.
- [5] OGANOV A. R. and GLASS C. W., *J. Chem. Phys.*, **124** (2006) 244704.
- [6] OGANOV A. R., LYAKHOV A. O. and VALLE M., *Acc. Chem. Res.*, **44** (2011) 227.
- [7] LYAKHOV A. O. *et al.*, *Comput. Phys. Commun.*, **184** (2013) 1172.
- [8] PERDEW J. P., BURKE K. and WANG Y., *Phys. Rev. B*, **54** (1996) 16533.
- [9] GIANOZZI P. *et al.*, *J. Phys.: Condens. Matter*, **21** (2009) 395502.
- [10] TROULLIER N. and MARTINS J. L., *Phys. Rev. B*, **43** (1991) 1993.
- [11] PRELOG V. and SEIWERTH R., *Berichte*, **74** (1941) 1644.
- [12] FISCHER J., BAUMGARTNER J. and MARSCHNER C., *Science*, **310** (2005) 825.
- [13] FEHÉR F., SCHINKITZ D. and SCHAAF J. Z., *Anorg. Allg. Chem.*, **383** (1971) 303.
- [14] GE Y. and HEAD J. D., *J. Phys. Chem. B*, **106** (2002) 6997.
- [15] BYRD R. H., HRIBAR M. E., and NOCEDAL J., *SIAM J. Optim.*, **89** (1999) 247.
- [16] PIETRUCCI F. and ANDREONI W., *Phys. Rev. Lett.*, **107** (2011) 085504.
- [17] GLANSDORFF P. and PRIGOGINE I., *Thermodynamic Theory of Structure, Stability, and Fluctuations* (Wiley-Interscience, New-York) 1971, sect. 4.2.